JOURNAL OF APPLIED PHYSICS VOLUME 90, NUMBER 10 15 NOVEMBER 2001

Nearly 100% internal phosphorescence efficiency in an organic light emitting device

Chihaya Adachi, Marc A. Baldo, Mark E. Thompson,[a] and Stephen R. Forrest
Center for Photonics and Optoelectronic Materials (POEM), Department of Electrical Engineering, Princeton University, Princeton, New Jersey 08544

(Received 8 May 2001; accepted for publication 13 August 2001)

We demonstrate very high efficiency electrophosphorescence in organic light-emitting devices employing a phosphorescent molecule doped into a wide energy gap host. Using bis(2-phenylpyridine)iridium(III) acetylacetonate $[(\mathrm{ppy})_2\mathrm{Ir(acac)}]$ doped into 3-phenyl-4-(1′-naphthyl)-5-phenyl-1,2,4-triazole, a maximum external quantum efficiency of (19.0±1.0)% and luminous power efficiency of (60±5) lm/W are achieved. The calculated internal quantum efficiency of (87±7)% is supported by the observed absence of thermally activated nonradiative loss in the photoluminescent efficiency of $(\mathrm{ppy})_2\mathrm{Ir(acac)}$. Thus, very high external quantum efficiencies are due to the nearly 100% internal phosphorescence efficiency of $(\mathrm{ppy})_2\mathrm{Ir(acac)}$ coupled with balanced hole and electron injection, and triplet exciton confinement within the light-emitting layer.

[DOI: 10.1063/1.1409582]

I. INTRODUCTION

Inorganic, direct band gap semiconductor heterostructure light-emitting devices and lasers comprised of III–V compounds based on GaAs and InP, are known to have nearly 100% internal quantum efficiency (η_{int}).[1] Since holes and electrons in the valence and conduction bands, respectively, are considered as free particles, radiative and nonradiative transitions in these direct band gap materials do not involve the intermediate formation of excitons. In contrast, many optical processes in organic thin films are mediated by excitons which can ultimately lead to a reduction in electroluminescence efficiency in polymer and molecular organic light emitting devices (OLEDs). Besides nonradiative pathways due to strong exiton–phonon coupling, the fraction of singlet excitons (χ) under electrical excitation is 0.25 in a molecular solid such as aluminum tris(8-hydroxyquinoline) (Alq_3),[2] limits η_{int} to only 25% when fluorescence-based light emitting molecules are employed. The OLED external quantum efficiency (η_{ext}) follows:

$$\eta_{\mathrm{ext}}=\eta_{\mathrm{int}}\eta_{\mathrm{ph}}=\gamma\eta_{\mathrm{ex}}\phi_p\eta_{\mathrm{ph}}, \tag{1}$$

where η_{ph} is the light out-coupling efficiency, η_{ex} is the fraction of total excitons formed which result in radiative transitions ($\eta_{\mathrm{ex}}\sim 1/4$ for fluorescent molecular dyes, and 1 for phosphorescent materials), γ is the ratio of electrons to holes (or vice versa, to maintain $\gamma\leqslant 1$) injected from opposite contacts (the electron–hole charge-balance factor), and ϕ_p is the intrinsic quantum efficiency for radiative decay (including both fluorescence and phosphorescence). If only singlets are radiative in fluorescent materials, η_{ext} is limited to ~5%, assuming[3] $\eta_{\mathrm{ph}}\sim 1/2n^2\sim 20\%$ for a glass substrate with index of refraction $n=1.5$. In contrast, by using high efficiency phosphorescent materials which harvest both singlet and triplet excitons, η_{int} can approach 100%, in which case we can anticipate $\eta_{\mathrm{ext}}\sim 20\%$.

The recent fabrication of extremely efficient electrophosphorescent OLEDs employing Pt and Ir complexes suggests that devices with internal quantum efficiencies of 100% are achievable through radiative recombination of both singlet and triplet excitons.[4–13] Attempts to observe electrophosphorescence (EP) were reported using keto-coumarin[14] and benzophenone[15] derivatives. The efficiency of these materials was low, $\eta_{\mathrm{ext}}<1\%$, even at 77 K, because the rate of phosphorescent light emission was comparable to the excited state nonradiative decay rate. However, organometallic compounds which introduce spin–orbit coupling due to the central heavy metal atom show a relatively high ligand based phosphorescence efficiency ($\phi_p>20\%$) even at room temperature because of the strong radiative transition moment of $n-\pi^*$, $\pi-\pi^*$ and the metal-to-ligand charge transfer states.[12] Using this approach, demonstrations of high-efficiency ($\eta_{\mathrm{ext}}>5\%$) OLEDs were made possible using 2,3,7,8,12,13,17,18-octaethyl-21*H*,23*H*-porphine platinum (II),[4,5] and *fac* tris(2-phenylpyridine)iridium $[\mathrm{Ir(ppy)}_3]$ and its derivatives.[6–13]

Here, we demonstrate very high efficiency EP-OLEDs employing the green electrophosphorescent molecule, bis(2-phenylpyridine) iridium(III)acetylacetonate $[(\mathrm{ppy})_2\mathrm{Ir(acac)}]$, with a maximum $\eta_{\mathrm{ext}}=(19.0\pm 0.5)\%$ and luminous power efficiency of $\eta_p=(60\pm 5)$ lm/W.[16] We show that these values correspond to $\eta_{\mathrm{int}}=(87\pm 7)\%$. We also demonstrate that the very high internal quantum efficiency is due to direct exciton formation at the guest phosphor, along with subsequent exciton confinement within the emissive layer.

II. EXPERIMENTAL METHOD

Organic layers were deposited by high-vacuum (10^{-6} Torr) thermal evaporation onto a clean glass substrate pre-

---

[a] Present address: Department of Chemistry, University of Southern California, Los Angeles, CA 90089.

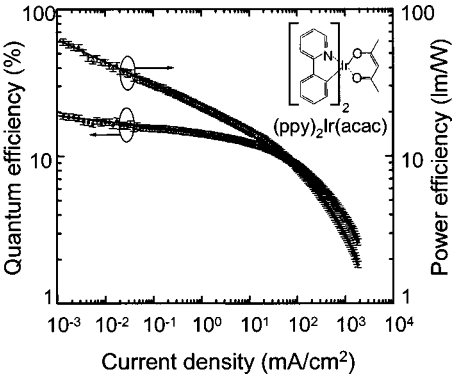

FIG. 1. The external quantum and power efficiencies of an ITO/HMTPD (60 nm)/12%-(ppy)$_2$Ir(acac):*TAZ* (25 nm)/Alq$_3$ (50 nm)/Mg:Ag/Ag OLED. A maximum external quantum efficiency of $\eta_{\text{ext}} = (19.0 \pm 0.5)\%$ and power efficiency of $\eta_p = (60 \pm 5)$ lm/W were obtained. Inset: Molecular structure of (ppy)$_2$Ir(acac).

coated with an indium tin oxide (ITO) layer (160 mm thick) with a sheet resistance of ~20 Ω/sq. Prior to use, the substrate was degreased with solvents and cleaned in a UV-ozone chamber before it was loaded into the evaporation system. First, a 60 nm thick hole transport layer of 4,4′-bis[N,N′-(3-tolyl)amino]-3,3′-diemthyl biphenyl (HMTPD)[8] was deposited, followed by a 25 nm thick light-emitting layer (EML) consisting of[17] (ppy)$_2$Ir(acac) codeposited with[8] a 3-phenyl-4-(1′-naphthyl)-5-phenyl-1,2,4-triazole (TAZ) electron-transport host layer. A 50 nm thick layer of Alq$_3$ was then deposited onto the EML surface to transport and inject electrons into the EML. A shadow mask with 1 mm diameter openings was used to define the cathode consisting of a 150 nm thick Mg:Ag (10:1) layer, with a 20 nm thick Ag cap. Similar results to those reported here were also obtained employing a LiF/Al cathode.

Current density (*J*)–voltage (*V*)–luminance (*L*) characteristics were measured using an HP4145B semiconductor parameter analyzer, with the quantum efficiency directly obtained by placing the OLED approximately 3 mm above the center of a large diameter (1.13 cm) calibrated Si photodiode. Since almost all of the emitted light from the OLED substrate surface is detected by the photodiode, this method avoids systematic errors introduced by corrections needed to account for non-Lambertian spatial emission patterns.[7] Furthermore, this direct measurement of the quantum efficiency also eliminates errors often introduced by first measuring device luminance and then converting the data to efficiency after determination of the OLED emission spectrum.[18]

III. RESULTS

Figure 1 shows the EP-OLED efficiency with 12%-(ppy)$_2$Ir(acac) doped into TAZ. A maximum $\eta_{\text{ext}} = (19.0 \pm 0.5)\%$ and $\eta_p = (60 \pm 5)$ lm/W are obtained at a current of $J = 1.5$ μA/cm^2 and luminance of 1.3 cd/m^2. The device exhibits a gradual decrease in η_{ext} with increasing current at $J > 10$ mA/cm^2 due to triplet–triplet annihilation.[19,20] Even at a luminance of ~1000 cd/m^2 corresponding to $J = 2.1$ mA/cm^2, $\eta_{\text{ext}} = (13.7 \pm 0.5)\%$ was observed.

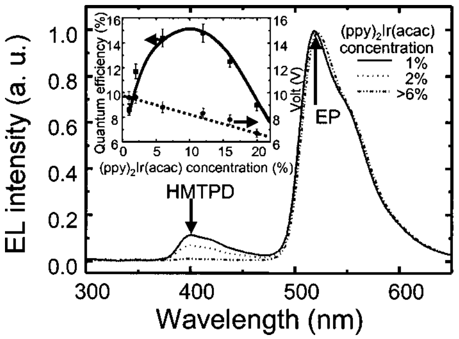

FIG. 2. Concentration dependence of EL spectra on (ppy)$_2$Ir(acac) of an ITO/HMTPD (60 nm)/1%, 2%, and 6%-(ppy)$_2$Ir(acac):TAZ (25 nm)/Alq$_3$ (50 nm)/Mg:Ag/Ag OLED. Inset: Concentration dependence of the external quantum efficiency (η_{ext}) and driving voltage of a (ppy)$_2$Ir(acac) device with a structure: ITO/HMTPD (60 nm)/*X*%-(ppy)$_2$Ir(acac):TAZ (25 nm)/Alq$_3$ (50 nm) Mg:Ag/Ag ($X = 1\%$ to 20%).

Figure 2 shows the dependence of the (ppy)$_2$Ir(acac) EP spectrum on doping concentration in TAZ. At concentrations >6%, we only observe the electroluminescence (EL) component centered at a wavelength of $\lambda = 520$ nm due to the (ppy)$_2$Ir(acac) phosphorescence. At (ppy)$_2$Ir(acac) concentrations less than 2%, an additional deep blue emission ($\lambda = 395$ nm) due to HMTPD fluorescence is also observed. The inset of Fig. 2 shows (ppy)$_2$Ir(acac) concentration dependences of η_{ext} and drive voltage at 1 mA/cm^2. A maximum η_{ext} was observed at (ppy)$_2$Ir(acac) concentrations from 5% to 12%, while a significant decrease in η_{ext} was observed at both higher and lower concentrations. In addition, a gradual decrease of the drive voltage was observed with an increase in (ppy)$_2$Ir(acac) concentration.

We also measured the temperature dependence of the EP and photoluminescence (PL) quantum efficiencies of the EML from $T = 15$ to 300 K. Figure 3 shows the temperature dependence of the PL spectra in a (ppy)$_2$Ir(acac) doped TAZ film. The temperature dependencies of the integrated PL and EP intensities under a constant current density of $J = 0.1$ mA/cm^2 are shown in the insets of Fig. 3. While the spectral width decreased slightly with temperature, both the PL and EP intensities are temperature independent.

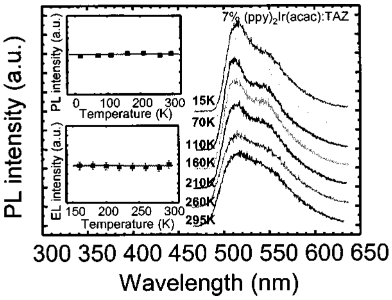

FIG. 3. Temperature dependence of the PL spectrum of a 12%-(ppy)$_2$Ir(acac):TAZ film from $T = 275$ to 15 K. Inset: Temperature dependence of the PL intensity of a 12%-(ppy)$_2$Ir(acac):TAZ film and EP intensity of the OLED at $J = 0.1$ mA/cm^2.

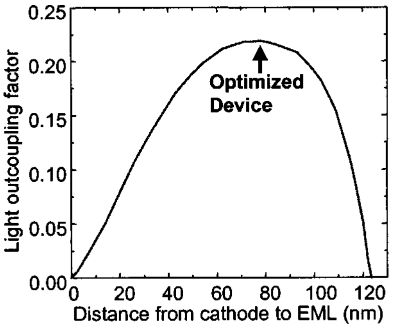

FIG. 4. Calculated light out-coupling factor for glass ($n=1.5$)/ITO (160 nm)/organic layer (125 nm)/Mg:Ag/Ag. The abscissa shows the distance of the light emitting layer from the Mg:Ag cathode.

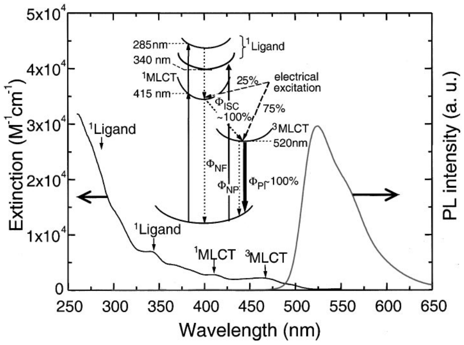

FIG. 5. Absorption and emission spectra of $(ppy)_2Ir(acac)$. Inset: Energy level diagram of $(ppy)_2Ir(acac)$. The ligand singlet (^{1}Ligand) and triplet (^{3}Ligand) states, (^{1}MLCT) and (^{3}MCLT) were determined from the absorption and emission spectra. Φ_{NF}, Φ_{ISC}, Φ_{PI}, and Φ_{NP} are quantum yields for nonemissive transitions from ^{1}MLCT intersystem crossing, intrinisc phosphorescent transitions, and nonemissive transitions from ^{3}MLCT, respectively.

IV. DISCUSSION

A. Internal electrophosphorescent quantum efficiency

To determine the internal quantum efficiency of the EP-OLED, we begin by calculating the radiative modes in the OLED optical microcavity[21,22] employing the theory of Chance *et al.*[23] Dyadic Green's functions are used to compute the radiative decay rates, allowing us to consider arbitrarily complex structures. This treatment also accounts for nonradiative losses due to dipole coupling with surface plasmon modes at the metalorganic cathode interface. We model the OLED in Fig. 1 as a four-layer structure: the Mg:Ag cathode is considered semi-infinite with a refractive index of $n_{\mathrm{Mg}}=0.25+i4.36$;[24] the organic layers are represented by a single layer of thickness 125 nm with refractive index $n=1.7$;[21] the ITO has a thickness of 160 nm and a refractive index of $n=1.9+i0.01$,[25] where the absorption was calculated from transmission measurements; and finally the semi-infinite glass layer has a refractive index of $n=1.5$. The glass substrate is approximately 1 mm thick, allowing for the use of ray optics to calculate the angular emission pattern within the glass, and consequently the coupling into air. For luminescence at the HMTPD $(ppy)_2Ir(acac)$:TAZ interface 75 nm from the cathode, we calculate an output coupling efficiency of $\eta_p=(22\pm2)\%$ (Fig. 4). Hence, for $\eta_{\mathrm{ext}}=(19.0\pm0.5)\%$, we obtain $\eta_{\mathrm{int}}=(87\pm7)\%$.

With our estimate of η_{int}, we can infer the efficiencies of the molecular transitions leading to EP using Fig. 5, which shows the absorption and emission spectra of $(ppy)_2Ir(acac)$ identifying transitions from several excited state manifolds. The energy level scheme inferred from these spectra is shown in the inset. Phosphorescence proceeds via either direct injection into the triplet metal ligand charge transfer state (^{3}MLCT), or via intersystem crossing (ISC) from the singlet charge transfer state (^{1}MLCT). Now, the phosphorescence quantum yield (ϕ_p) follows:

$$\phi_p=\kappa_p/[\kappa_p+\kappa_{\mathrm{NP}}], \tag{2}$$

where κ_p is the phosphorescence emission rate and κ_{NP} that of nonemissive triplet decay. Under electrical excitation, on the other hand, both singlet and triplet excitons are directly created on either the guest or host molecules with a statistical splitting of $\chi=25\%$ singlets and $(1-\chi)=75\%$ triplets.[2] Thus, η_{int} follows [c.f. Eqs. (1) and (2)]:

$$\eta_{\mathrm{int}}=\gamma\phi_p\eta_{\mathrm{ex}}=\gamma\kappa_p/[\kappa_p+\kappa_{\mathrm{NP}}][(1-\chi)+\chi\phi_{\mathrm{ISC}}]. \tag{3}$$

From the temperature independence of the PL and EP efficiencies (see inset of Fig. 3), we infer that the temperature-dependent nonradiative pathways are almost negligible in a $(ppy)_2Ir(acac)$:TAZ solid-state film even at room temperature. Note, however, that some nonradiative processes (e.g., triplet–triplet and triplet–polaron annihilation, and field-dependent exciton dissociation, etc.) do not depend strongly on temperature. From our measurements of $\eta_{\mathrm{int}}=(87\pm7)\%$, Eq. (3) implies that the $(13\pm7)\%$ loss in total efficiency must arise either from residual nonradiative processes in $(ppy)_2Ir(acac)$ or because ϕ_{ISC} or γ is less than 1. However, it is unlikely that $\phi_{\mathrm{ISC}}<1$ since, in that case, we would anticipate fluorescent emission from the ^{1}MCLT to ground state on a time scale of ~10 ns, but this emission is not observed at any temperature or pumping intensity used in these studies. Hence, we conclude that both the photoluminescent efficiency of $(ppy)_2Ir(acac)$ and γ are at least ~0.9.

B. Exciton formation process

The EP spectral characteristics in Fig. 2 suggest that at $(ppy)_2Ir(acac)$ concentrations less than 2%, hole injection from the HMTPD highest occupied molecular orbital (HOMO) into the TAZ HOMO is energetically unfavorable, and carrier recombination partly occurs within HMTPD [c.f. energy level diagram in Fig. 6(a)]. The large energy difference between the HOMO level of HMTPD and TAZ of ~1.0 eV prevents direct hole injection from HMTPD into TAZ. The accumulated holes at the interface then recombine with electrons injected from TAZ layer, leading to blue HMTPD emission in addition to exciton formation at $(ppy)_2Ir(acac)$. This analysis is consistent with the dominant electron transport characteristics of TAZ. At $(ppy)_2Ir(acac)$ concentrations higher than 6%, on the other hand, there is no HMTPD blue emission (Fig. 2). Thus, we conclude that $(ppy)_2Ir(acac)$ exciton formation occurs directly on $(ppy)_2Ir(acac)$ from holes injected from HMTPD and electrons primarily transported at the TAZ lowest unoccupied molecular orbital (LUMO) energy [Fig. 6(b)]. A decrease of the driving voltage with in-

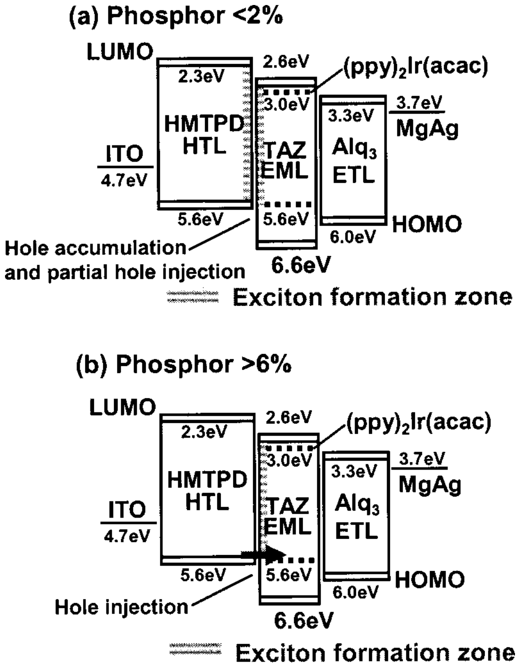

FIG. 6. Energy diagrams of the ITO/HMTPD/((ppy)$_2$Ir(acac):TAZ/Alq$_3$/MgAg/Ag EP-OLED showing the relative positions of the HOMO and LUMO levels of the various organic layers, corresponding to dopant concentrations of (a) $<2\%$ (ppy)$_2$Ir(acac) and (b) $>6\%$ (ppy)$_2$Ir(acac) in a TAZ host.

creasing phosphor concentration is evident for the direct hole injection process. Since the HOMO levels of HMTPD and (ppy)$_2$Ir(acac) are aligned at 5.6 eV, direct hole injection at the HMTPD/EML interface should reduce the drive voltage, as observed.

Recall that the electron–hole charge-balance factor, $\gamma \lesssim 0.9$. Since most holes injected into the (ppy)$_2$Ir(acac) HOMO level recombine with electrons at this interface, and since hole transport in the doped TAZ layer is probably more likely than electron transport through the HMTPD HTL, we speculate that the hole density is slightly higher than that of electrons, possibly leading to deviation in γ from its ideal value of 1. After direct exciton formation on (ppy)$_2$Ir(acac), the exciton radiatively decays due to the wide energy gap of a TAZ host which confines triplet excitons on the guest molecule. No host fluorescence and phosphorescence even at a low temperature thus ensures good exciton confinement on the phosphor guest.

V. SUMMARY

In conclusion, we demonstrated a very high-efficiency EP-OLED approaching 100% internal quantum efficiency. The high internal phosphorescence efficiency and charge balance in the structure are responsible for the high efficiency. From these results, we find that further increases in OLED efficiency will only be obtained by developing schemes for increasing light out-coupling by incorporating microcavities,[21,26] shaped substrates,[27,28] or an index matching medium[29,30] in combination with the use of phosphorescent molecular dyes.

ACKNOWLEDGMENTS

The authors are grateful to Universal Display Corporation, the National Science Foundation MRSEC program, and the Defense Advanced Research Projects Agency for their support of this research.

[1] L. A. Coldren and S. W. Corzine, *Diode Lasers and Photonic Integrated Circuits* (Wiley, New York, 1995), p. 54.
[2] M. A. Baldo, D. F. O'Brien, M. E. Thompson, and S. R. Forrest, Phys. Rev. B **60**, 14422 (1999).
[3] N. C. Greenham, R. H. Friend, and D. D. C. Bradley, Adv. Mater. **6**, 491 (1994).
[4] M. A. Baldo, D. F. O'Brien, Y. You, A. Shoustikov, S. Sibley, M. E. Thompson, and S. R. Forrest, Nature (London) **395**, 151 (1998).
[5] D. F. O'Brien, M. A. Baldo, M. E. Thompson, and S. R. Forrest, Appl. Phys. Lett. **74**, 442 (1999).
[6] M. A. Baldo, S. Lamansky, P. E. Burrows, M. E. Thompson, and S. R. Forrest, Appl. Phys. Lett. **75**, 4 (1999).
[7] T. Tsutsui, M. J. Yang, M. Yahiro, K. Nakamura, T. Watanabe, T. Tsuji, Y. Fukuda, T. Wakimoto, and S. Miyaguchi, Jpn. J. Appl. Phys., Part 2 **38**, L1502 (1999).
[8] C. Adachi, M. A. Baldo, and S. R. Forrest, Appl. Phys. Lett. **77**, 904 (2000).
[9] C.-L. Lee, K. B. Lee, and J.-J. Kim, Appl. Phys. Lett. **77**, 2280 (2000).
[10] C. Adachi, M. A. Baldo, S. R. Forrest, S. Lamansky, M. E. Thompson, and R. C. Kwong, Appl. Phys. Lett. **78**, 1622 (2001).
[11] C. Adachi, M. A. Baldo, M. E. Thompson, and S. R. Forrest, Bull. Am. Phys. Soc. **46**, 863 (2001).
[12] S. Lamansky, P. Djurovich, D. Murphy, F. Abdel-Razzaq, C. Adachi, P. E. Burrows, S. R. Forrest, and M. E. Thompson, J. Am. Chem. Soc. **123**, 4304 (2001).
[13] C. Adachi, R. C. Kwong, and S. R. Forrest, Organic Electronics **2**, 37 (2001).
[14] M. Morikawa, C. Adachi, T. Tsutsui, and S. Saito, 51st Fall Meeting, Jpn. Soc. Appl. Phys., Paper 28a-PB-8 (1990).
[15] S. Hoshino and H. Suzuki, Appl. Phys. Lett. **69**, 224 (1996).
[16] These results are similar to those recently reported for OLEDs employing the analogous phosphor, Ir(ppy)$_3$ doped into a hole-transporting host by M. Ikai, S. Tokito, Y. Sakamoto, T. Suzuki, and Y. Taga, Appl. Phys. Lett. **79**, 156 (2001).
[17] S. Lamansky, P. Djurovich, D. Murphy, F. Abdel-Razaq, R. Kwong, I. Tsyba, M. Bortz, B. Mui, R. Bau, and M. E. Thompson, Inorg. Chem. **40**, 1704 (2001).
[18] J. Kido and Y. Iizumi, Appl. Phys. Lett. **73**, 2721 (1998).
[19] C. Adachi, M. A. Baldo, and S. R. Forrest, J. Appl. Phys. **87**, 8049 (2000).
[20] M. A. Baldo, C. Adachi, and S. R. Forrest, Phys. Rev. B **62**, 10967 (2000).
[21] V. Bulovic, V. B. Khalfin, G. Gu, P. E. Burrows, D. Z. Garbuzov, and S. R. Forrest, Phys. Rev. B **58**, 3730 (1998).
[22] J-S Kim, P. K. H. Ho, N. C. Greenham, and R. H. Friend, J. Appl. Phys. **88**, 1073 (2000).
[23] R. R. Chance, A. Prock, and R. Sibley, Adv. Chem. Phys. **37**, 1 (1978).
[24] *Handbook of Optical Constants of Solids* (Academic, Orlando, FL, 1985).
[25] J. S. Kim, P. K. H. Ho, N. C. Greenham, and R. H. Friend, J. Appl. Phys. **88**, 1073 (2000).
[26] R. H. Jordan, L. J. Rothberg, A. Dodabalapur, and R. E. Slusher, Appl. Phys. Lett. **69**, 1997 (1996).
[27] G. Gu, D. Z. Garbuzov, P. E. Burrows, S. Venkatesh, and S. R. Forrest, Opt. Lett. **22**, 396 (1997).
[28] C. F. Madigan, M. H. Lu, and J. C. Sturm, Appl. Phys. Lett. **76**, 1650 (2000).
[29] M. Borodilsky, T. F. Kraus, R. Coccioli, R. Vrijen, R. Bhat, and E. Yablonovitch, Appl. Phys. Lett. **75**, 1036 (1999).
[30] T. Yamazaki, K. Sumioka, and T. Tsutsui, Appl. Phys. Lett. **76**, 1243 (2000).